

Investigating potential ferroptosis-related differentially expressed genes and biomarkers of ischemic stroke in elderly women using bioinformatics

S. LI¹, Z.-Y. LI², L.-H. QIN^{2,3}

¹School of Informatics, ²School of Nursing, ³Key Laboratory of Hunan Province for Prevention and Treatment of Integrated Traditional Chinese and Western Medicine on Cardiocerebral Diseases, Hunan University of Chinese Medicine, Changsha, China

Sheng Li and Ziyang Li contributed equally to this study and are considered as co-first authors

Abstract. – **OBJECTIVE:** Women have a higher lifetime risk of stroke than men and are more likely to die from it. Ferroptosis is a recently discovered form of programmed cell death implicated in many diseases. The role of ferroptosis-related genes in the diagnosis, prognosis, and treatment of elderly women with ischemic stroke (IS) requires additional clarification. This paper aimed to screen ferroptosis-related genes associated with IS in elderly women and to identify hub genes and candidate drugs.

MATERIALS AND METHODS: Ferroptosis-related differentially expressed genes (DEGs) in elderly women with IS were identified by bioinformatics analysis of the GSE22255 and ferroptosis-related gene datasets. Subsequently, ferroptosis-related hub genes were used to predict targeted miRNA, construct the miRNA-mRNA network, and identify candidate drugs.

RESULTS: Eleven ferroptosis-related DEGs were identified in elderly women with IS vs. controls. Gene Ontology and Kyoto Encyclopedia of Genes and Genomes analysis revealed that the 11 genes were mainly enriched in the IL-17, TNF, and NF- κ B signaling pathways. Moreover, the hub genes suggested 10 ferroptosis-related biomarkers for IS, including *SOCS1*, *IFNG*, *TNFAIP3*, *IL1B*, *IL-6*, *PTGS2*, *DDIT3*, *CXCL2*, *NFE2L2*, and *ATF3*. Furthermore, our findings revealed the miRNA-mRNA network of the hub genes and identified candidate drugs. 10 potential therapeutic compounds, especially estradiol CTD 00005920, corresponded to the 10 key genes which could be targets for IS treatment in elderly women.

CONCLUSIONS: Our results suggested ferroptosis-related DEGs (*SOCS1*, *IFNG*, *TNFAIP3*, *IL1B*, *IL-6*, *PTGS2*, *DDIT3*, *CXCL2*, *NFE2L2*, and

ATF3) as potential biomarkers for IS diagnosis, prognosis, and treatment, providing additional evidence of the important role of ferroptosis in IS in elderly women.

Key Words:

Ferroptosis, Ischemic stroke, Elderly women, Biomarker, Bioinformatics.

Introduction

Stroke is a leading cause of death and disability globally¹, with ischemic stroke (IS) accounting for approximately 87% of all strokes². Major risk factors of IS include age, sex, ethnicity, genetics, hypertension, diabetes mellitus, smoking, metabolic syndrome, and atrial fibrillation³. Women have an approximately 4% higher lifetime stroke risk⁴ and have worse outcomes and higher mortality than that in men⁵. This is attributable to female-specific risk factors, such as menopause, delayed recognition of the condition, and treatment delay⁶. In contrast, there is increasing evidence⁷ that early the diagnosis of IS can improve the therapeutic effect and prognosis for patients. It suggests the importance of clarifying the potential mechanisms of IS in elderly women to identify new biomarkers and therapeutic targets.

Dixon et al⁸ first reported ferroptosis, a novel form of programmed cell death characterized by intracellular iron accumulation and lipid peroxidation. Morphologically, ferroptosis is characterized by an intact cell membrane, reduced cell volume,

increased mitochondrial membrane density, the disappearance of mitochondrial cristae, mitochondrial membrane contraction, mitochondrial outer membrane rupture, a normal nucleus size, and the lack of chromatin concentration^{8,9}. Ferroptosis can be regulated by multiple proteins and genes, and it involves various metabolic pathways, including iron, amino acid, and lipid metabolism. Ferroptosis is ubiquitous in human bodies because it functions in physiological and pathogenic processes. Recent evidence¹⁰ suggests that ferroptosis is related to diseases such as atherosclerosis (AS), ischemia-reperfusion injury, and stroke. However, the role of ferroptosis-related genes in the diagnosis, prognosis, or treatment of IS in elderly women has not been fully clarified.

Therefore, this study aimed to investigate the role of ferroptosis in elderly women with IS. Using bioinformatics, this study applied the Gene Expression Omnibus (GEO) dataset GSE22255 to identify the differentially expressed genes (DEGs) in elderly women with IS. The intersecting genes, DEGs of the GSE22255 dataset, and ferroptosis-related genes of the FerrDb database were considered the ferroptosis-related DEGs. Finally, these common genes were analyzed to determine their main biological functions and to perform enrichment analysis. Meanwhile, through protein-protein interaction (PPI) and cytoHubba analysis, key IS-associated genes were identified and predicted based on miRNA and target drug prediction. The results could provide a molecular theoretical basis for diagnostic and therapeutic biomarkers of IS.

Materials and Methods

Ferroptosis-Related Gene Database

The assembled set of ferroptosis-related genes was retrieved from the FerrDb database (<http://www.zhounan.org/ferrdb>)¹¹, including the gene and chemical substance categories of the ferroptosis regulators. The gene regulators included drivers, suppressors, and markers, and the chemical substance regulators included inducers and inhibitors. FerrDb consists of six independent datasets.

Dataset Collection and Processing

The GSE22255 dataset illustrates the genomic expression profiles of peripheral blood mononuclear cells (PBMCs) from IS patients compiled from the GEO database. The platform was the

GPL570 [HG-U133_Plus_2] Affymetrix Human Genome U133 Plus 2.0 Array. The IS dataset (GSE22255) contains data from PBMCs of 20 IS patients and 20 sex- and age-matched controls. The study selected five samples of elderly women with IS (≥ 60 years old) and five sex- and age-matched control samples. The ‘Umap’ (version 0.2.7.0) and ‘ggplot2’ (version 3.3.3) packages of R (version 3.6.3, <https://cran.r-project.org/index.html>) were used for statistical analysis and visualization, including the development of box diagrams of normalized samples, principal component analysis (PCA), and Umap visualisation.

Differential Analysis

First, we combined the data of the six independent FerrDb datasets. Then, DEGs between the five samples of elderly women with IS and the control group were analyzed and visualized using the ‘ggplot2’ and ‘ComplexHeatmap’ packages of R software (version 3.6.3)¹². Cut-off criteria were obtained for GSE22255 using the criteria $|\log_2(\text{fold change, FC})| > 1$ and $p.\text{adj} < 0.05$. Venn diagrams (<http://www.interactivenn.net>) were applied to find common DEGs between the GSE22255 dataset and the FerrDb database, which were visualized using volcano and heat maps.

Functional Enrichment Analysis

Gene ontology (GO) terms are organized into three categories, biological process (BP), molecular function (MF), and cellular component (CC)¹³. The analysis and visualization of GO and Kyoto Encyclopedia of Genes and Genomes (KEGG) databases were performed using logFC on the ‘org.Hs.eg.db’ (version 3.10.0), ‘GOplot’ (version 1.0.2), ‘clusterProfiler’ (version 3.14.3), and ggplot2 (version) packages¹⁴. The results were visualized using column, circle, and chord diagrams. The selection criteria were $p.\text{adj} < 0.05$ and $q\text{-value} < 0.2$.

PPI Establishment and Identification of Hub Genes

The PPI analysis of the DEGs was conducted using the Search Tool for the Retrieval of Interacting Genes/Proteins (STRING) database (version 11.0, <http://string-db.org>)¹⁵. In addition, a combined score > 0.4 was considered a statistically significant interaction. Then, Cytoscape software (version 3.7.1, <http://www.cytoscape.org>) was employed to visualize the resulting PPI network. The nodes correspond to proteins, and the edges represent the protein interactions.

Finally, the cytoHubba plugin in Cytoscape was applied to look for hub genes using the calculated degree of network topology.

Statistical Analysis

According to the data distribution, the expression of hub genes was statistically analyzed using either a *t*-test or Mann-Whitney U test. In addition, the Spearman correlation analysis was carried out for the hub genes, and the result was visualized using the ‘ggplot2’ package of R software. *p*-values <0.05 were considered statistically significant (all *p*-values presented are two-sided).

Ferroptosis-Related Hub Gene-Mediated Prediction of miRNA and Construction of the miRNA–mRNA Network

The miRNAs targeted by hub genes were predicted with miRwalk (version 3.0, <http://mirwalk.umm.uni-heidelberg.de/>). The selected genes targeting miRNAs were predicted using the miRWalk, miRDB, and TargetScan databases and were included in databases (miRDB or TargetScan database) other than the miRWalk database. Furthermore, the interaction network was visualized using Cytoscape software.

Identification of Candidate Drugs

Based on the hub genes, the targeting drugs were analysed with the Drug Signatures database (DSigDB). Access to the DSigDB database was acquired through the Enrichr (<https://amp.pharm.mssm.edu/Enrichr/>) platform.

Results

Evaluation of GEO Datasets

After data standardization, the median of the visualization diagram of each sample was basi-

cally a horizontal line (Figure 1, A1). In terms of sample clustering, the samples of two groups in the PCA and Umap diagram were separated (Figure 1, A2 and A3).

Analysis of Ferroptosis-Related DEGs

Eleven DEGs [suppressor of cytokine signalling 1 (*SOCS1*); interferon-gamma (*IFNG*); TNF alpha-induced protein 3 (*TNFAIP3*); interleukin-1 β (*IL1B*), nuclear receptor subfamily 1 group D member 2 (*NR1D2*); interleukin-6 (*IL-6*); prostaglandin-endoperoxide synthase 2 (*PTGS2*); DNA damage-inducible transcript 3 (*DDIT3*); CXC chemokine ligand 2 (*CXCL2*); nuclear factor erythroid 2-like 2 (*NFE2L2*); and activating transcription factor 3 (*ATF3*)] were found to be common between the GSE22255 datasets and FerrDb database (Table I and Figure 2, B1). This is displayed in the form of a volcanic plot and heat map (Figure 2, B2 and B3).

Functional Enrichment Analysis of Ferroptosis-Related DEGs

The current study analyzed GO terms and the KEGG pathways associated with the 11 common DEGs. Based on criteria of *p*.adj of <0.05 and *q*-value of < 0.2, there were 916 BPs, 6 CCs, 18 MFs, and 45 KEGG pathways were identified. The five most eminent GO terms included in the BP, MF, CC, and KEGG categories are presented in Table II and Figure 3.

PPI Network Construction and Ferroptosis-Related Hub Gene Identification

Based on the STRING database, the PPI network analysis of ferroptosis-related DEGs was performed and visualized with Cytoscape (Figure 4 D1). The top 10 genes, including *IL-6*, *IL1B*, *PTGS2*, *ATF3*, *CXCL2*, *TNFAIP3*, *NFE2L2*,

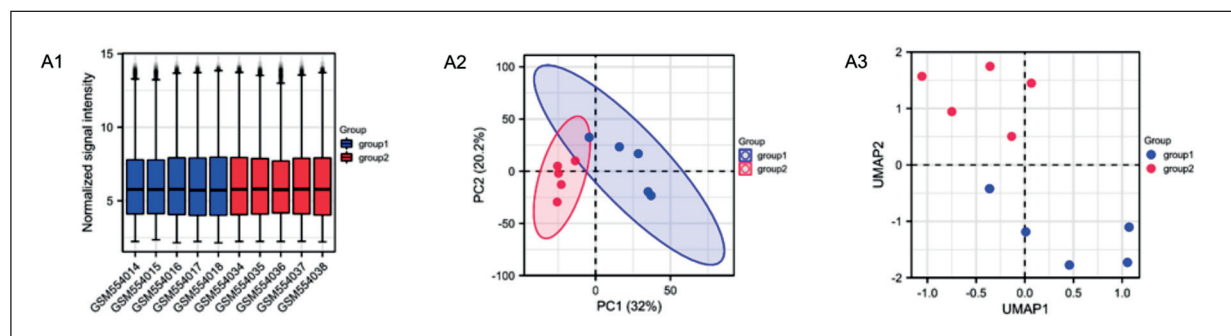


Figure 1. Evaluation of data in GSE22255 database. Group1 is the control group, and group2 is the experimental group. (A1) The normalized box diagram of the samples. (A2) The PCA diagram of two groups. (A3) The umap diagram of two groups.

Table I. The eleven differentially expressed ferroptosis-related DEGs in elderly women with IS compared to healthy controls.

ID	Gene symbol	logFC	p value	Adj. p value	Changes
210001_s_at	SOCS1	-1.505	$p \leq 0.001$	0.003	Down
210354_at	IFNG	-1.863	$p \leq 0.001$	0.005	Down
202644_s_at	TNFAIP3	-1.243	$p \leq 0.001$	0.030	Down
205067_at	IL1B	-3.064	$p \leq 0.001$	0.008	Down
209750_at	NR1D2	-1.196	$p \leq 0.001$	0.046	Down
205207_at	IL6	-5.050	$p \leq 0.001$	0.020	Down
204748_at	PTGS2	-2.714	$p \leq 0.001$	0.001	Down
209383_at	DDIT3	-1.199	$p \leq 0.001$	0.020	Down
209774_x_at	CXCL2	-3.080	$p \leq 0.001$	0.003	Down
201146_at	NFE2L2	-1.065	$p \leq 0.001$	0.013	Down
202672_s_at	ATF3	-1.844	$p \leq 0.001$	0.010	Down

DDIT3, *SOCS1*, and *IFNG*, were taken as potential hub genes via Cytoscape and are shown in Figure 4 D2 and Table III. *IL-6*, *IL1B*, and *PTGS2* (degree 18) were the most significantly enriched genes, followed by *ATF3* (degree 14); *CXCL2* and *TNFAIP3* (degree 12); and *NFE2L2*, *DDIT3*, *SOCS1*, and *IFNG* (degree 10), as shown in Table III.

Differential Expression of Ferroptosis-Related Hub Genes

The sample did not meet the normality test ($p < 0.05$); therefore, the Mann-Whitney U test was selected. The test showed that the expression of the 10 hub genes, *SOCS1*, *IFNG*, *TNFAIP3*, *IL1B*, *IL-6*, *PTGS2*, *DDIT3*, *CXCL2*, *NFE2L2*, and *ATF3* was significantly ($p < 0.01$) lower in group 2 than in group 1, as shown in Figure 5. Moreover, the expression of these markers was downregulated and verified in an IS cohort.

Correlation of Ferroptosis-Related the Hub Genes

Spearman correlation analysis was conducted for the 10 hub genes (Figure 6), and the results showed a positive correlation. All genes were correlated with each other.

Further miRNA Mining and Interaction Network Analysis

We analyzed the interaction of the hub genes with miRNAs. Figure 7 shows the interactions among the 10 hub genes and their target miRNAs.

Identification of Candidate Drugs

Using the Enrichr platform for identification and the DSigDB database for analysis, the candidate drugs were selected according to the ad-

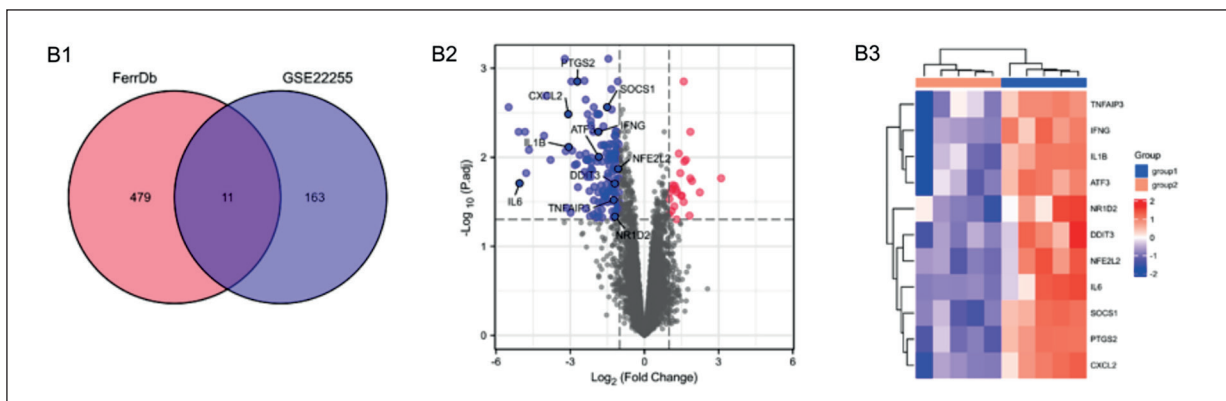


Figure 2. Analysis of Ferroptosis-Related DEGs. **B1**, The Venn map of intersection of ferroptosis-related genes and DEGs of GSE22255 dataset. **B2**, Volcano plot of ferroptosis-related DEGs between the elderly women with IS in the experimental group and the elderly women in the control group. Upregulated genes are marked with red dots, downregulated genes with blue dots, and genes without any significant difference are marked with gray dots. **B3**, Heat map of 11 ferroptosis-related DEGs between the elderly women with IS in the experimental group and the elderly women in the control group.

Table II. The top 5 GO/KEGG terms for ferroptosis-related DEGs in elderly women with IS.

Ontology	ID	Description	GeneRatio	BgRatio	<i>p</i> -value	<i>p. adjust</i>	<i>q</i> -value
BP	GO:2001233	Regulation of apoptotic signaling pathway	6/11	406/18670	4.29e-08	2.41e-05	6.90e-06
BP	GO:0150076	Neuroinflammatory response	4/11	75/18670	7.76e-08	2.41e-05	6.90e-06
BP	GO:0045073	Regulation of chemokine biosynthetic process	3/11	15/18670	6.90e-08	2.41e-05	6.90e-06
BP	GO:0042033	Chemokine biosynthetic process	3/11	16/18670	8.48e-08	2.41e-05	6.90e-06
BP	GO:0050755	Chemokine metabolic process	3/11	16/18670	8.48e-08	2.41e-05	6.90e-06
CC	GO:0090575	RNA polymerase II transcription factor complex	2/11	163/19717	0.004	0.031	0.019
CC	GO:0044798	Nuclear transcription factor complex	2/11	201/19717	0.005	0.031	0.019
CC	GO:0032993	Protein-DNA complex	2/11	202/19717	0.005	0.031	0.019
CC	GO:0005788	Endoplasmic reticulum lumen	2/11	309/19717	0.012	0.048	0.030
CC	GO:0005942	Phosphatidylinositol 3-kinase complex	1/11	27/19717	0.015	0.048	0.030
MF	GO:0005125	Cytokine activity	4/11	220/17697	7.16e-06	4.30e-04	1.88e-04
MF	GO:0005126	Cytokine receptor binding	4/11	286/17697	2.02e-05	6.05e-04	2.65e-04
MF	GO:0048018	Receptor ligand activity	4/11	482/17697	1.54e-04	0.003	0.001
MF	GO:0001228	DNA-binding transcription activator activity, RNA polymerase II-specific	3/11	439/17697	0.002	0.022	0.010
MF	GO:0000980	RNA polymerase II distal enhancer sequence-specific DNA binding	2/11	99/17697	0.002	0.022	0.010
KEGG	hsa04657	IL-17 signaling pathway	6/9	94/8076	1.73e-10	1.56e-08	7.28e-09
KEGG	hsa04668	TNF signaling pathway	5/9	112/8076	5.65e-08	2.54e-06	1.19e-06
KEGG	hsa05323	Rheumatoid arthritis	4/9	93/8076	1.99e-06	5.60e-05	2.62e-05
KEGG	hsa05146	Amoebiasis	4/9	102/8076	2.88e-06	5.60e-05	2.62e-05
KEGG	hsa04064	NF-kappa B signaling pathway	4/9	104/8076	3.11e-06	5.60e-05	2.62e-05

justed *p*-value. The result showed that the drug estradiol CTD 00005920 interacted with most genes. These landmark drugs were detected for the hub genes, representing common drugs that

can be used to treat ferroptosis-associated pathogenesis in elderly women with IS. Table IV shows the candidate drugs identified from the DsigDB database with respect to the hub genes.

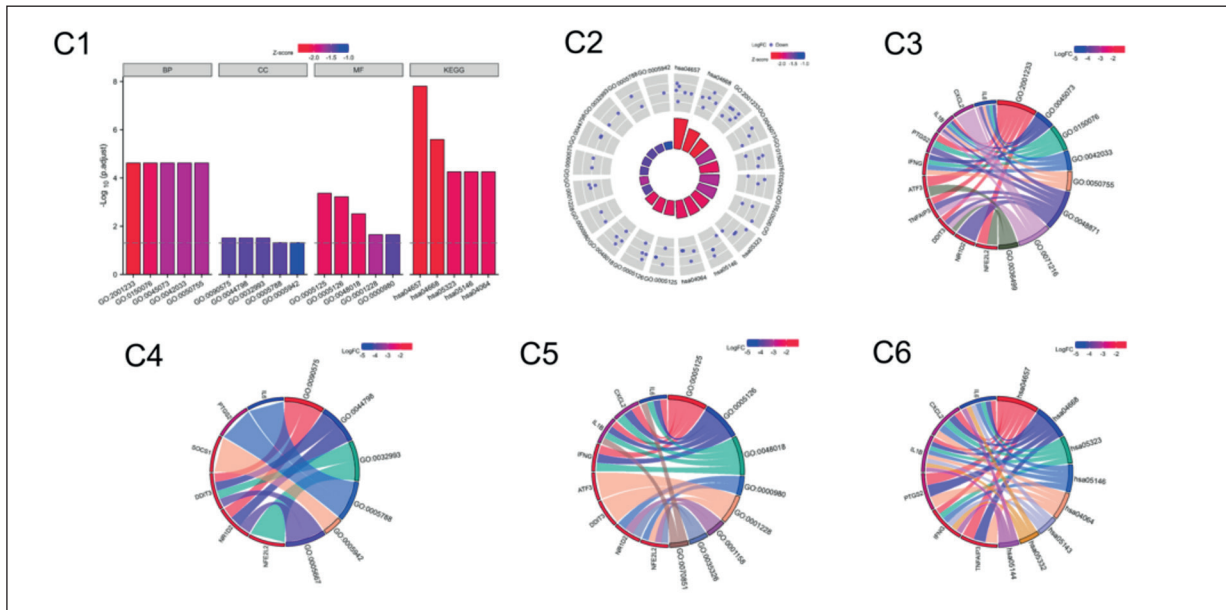


Figure 3. Enrichment analysis of ferroptosis-related DEGs in IS. **C1**, Column diagrams of GO and KEGG enrichment analysis. **C2**, Circle diagrams of GO and KEGG enrichment analysis. **C3**, Chord diagrams of BP. **C4**, Chord diagrams of CC. **C5**, Chord diagrams of MF. **C6**, Chord diagrams of KEGG.

Discussion

We first explored the DEGs in elderly women with IS vs. sex- and age-matched controls using the GSE22255 dataset, and then, compared them to a set of ferroptosis-related genes retrieved from the FerrDb database. Consequently, 11 ferroptosis-related DEGs were discovered in elderly women with IS. Moreover, GO and KEGG analyses revealed that these 11 ferroptosis-related DEGs were mainly enriched in the IL-17, TNF, and NF- κ B signaling pathways. Interestingly,

these genes and pathways were involved in IS. Through PPI construction and cytoHubba analysis, we identified 10 ferroptosis-related biomarkers for IS, namely, IL-6, IL1B, PTGS2, ATF3, CXCL2, TNFAIP3, NFE2L2, DDIT3, SOCS1, and IFNG.

IL-6, a key proinflammatory cytokine, participates in the pathological process of cerebral ischemia-reperfusion injury and is upregulated with transient middle cerebral artery occlusion¹⁶. In another study¹⁷, the expression of an inflammatory mediator cytokine, IL1B, was elevated

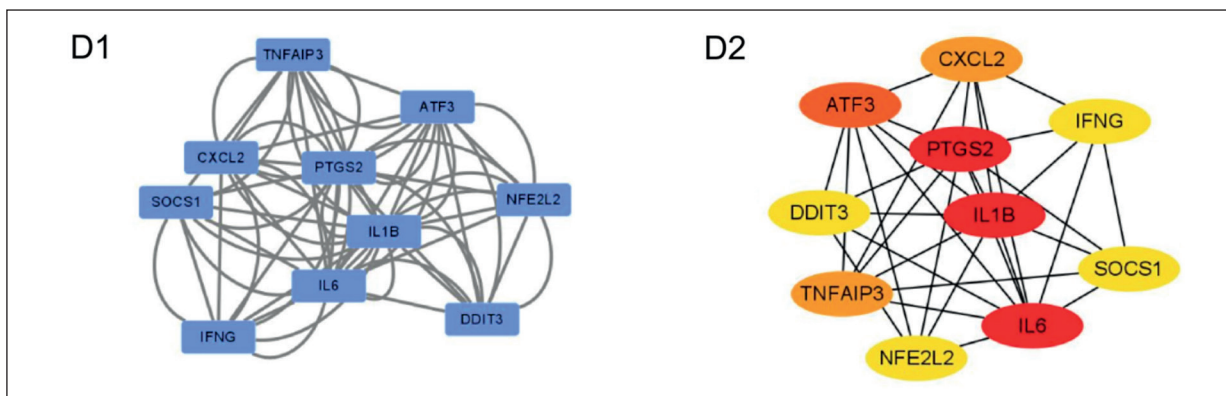


Figure 4. PPI network and ferroptosis-related hub gene. **D1**, PPI network of ferroptosis-related DEGs. **D2**, Ferroptosis-related hub genes.

Table III. Top ten in network edges ranked by Degree method.

Rank	Gene symbol	Score
1	IL6	18
1	IL1B	18
1	PTGS2	18
4	ATF3	14
5	CXCL2	12
5	TNFAIP3	12
7	NFE2L2	10
7	DDIT3	10
7	SOCS1	10
7	IFNG	10

upon early cerebral ischemia. IL-6 leads to the ferroptosis of cartilage cells by inducing cellular oxidative stress and altering iron homeostasis¹⁸. However, liproxstatin-1, a selective ferroptosis inhibitor, reduces microglia activation and IL-6 and IL1B release¹⁹. In this study, IL-6 and IL1B were involved in the IL-17, TNF, and NF-κB signaling pathways. Therefore, they were considered hub genes associated with ferroptosis in elderly women with IS.

PTGS2, known as cyclooxygenase-2, produces the inflammatory mediator prostaglandin E2 and is a rate-limiting enzyme in the biosynthesis of prostaglandins. The overexpression of PTGS2 also has a central role in IS pathogenesis. Moreover, the synthesis of inducible PTGS2 in the brain is activated by the NF-κB signaling pathway²⁰. Another study²¹ showed that PTGS2 as potential diagnostic biomarkers for IS. Additionally,

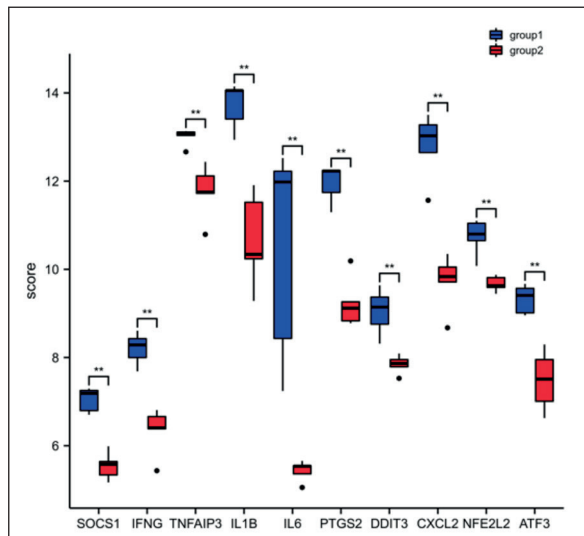


Figure 5. The expression of 10 ferroptosis-related hub genes. Blue represents group 1 (the control group), and red represents group 2 (the experimental group). * $p < 0.05$; ** $p < 0.01$.

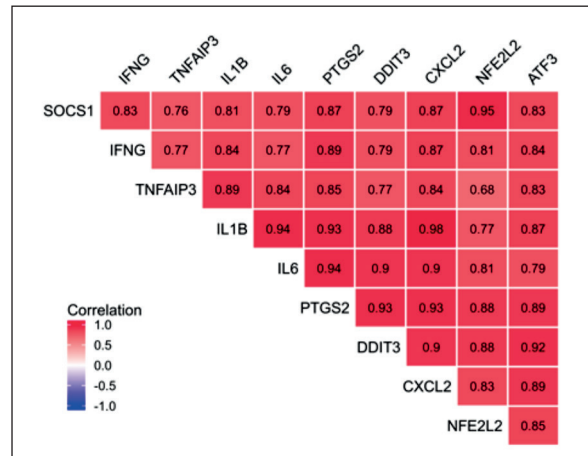


Figure 6. Correlation heatmap of ferroptosis-related hub genes. Red and blue represent positive correlation and negative correlation respectively of ten ferroptosis-related hub gene. The darker the color, the higher the correlation coefficient. The value represents the correlation coefficient, the larger the value, the stronger the correlation.

PTGS2 is a marker of ferroptosis²². These studies are consistent with our results, which identified PTGS2 as a hub gene of ferroptosis in elderly women with IS.

ATF3, as a transcription factor, is involved in the occurrence and regulation of ferroptosis and AS²³. Endoplasmic reticulum stress promotes an increase in intracellular H₂O₂ levels by upregulating ATF3. H₂O₂ increases intracellular Fe²⁺ and restricts glutathione synthesis, leading to the continuous accumulation of toxic intracellular lipid peroxides²⁴. ATF3 also promotes ferroptosis induced by erastin²⁵. The vulnerability of atherosclerotic plaques is one of the main causes of IS. These studies are consistent with our results, which also identified ATF3 as one of the hub genes of IS ferroptosis.

The mRNA levels of CXCL2 were found to increase significantly during plaque progression in a mouse AS model²⁶. In another study¹⁷, CXCL2 expression was significantly increased at 24h after brain ischemia induced by endothelin-1, but this increase returned to the baseline level after 48h. Similarly, in this study, CXCL2 was determined to be involved in ferroptosis and IS.

TNFAIP3 is a ubiquitin-modifying enzyme that is essential for the negative regulation of inflammation²⁷. Furthermore, TNF α-induced protein has been shown to negatively regulate the Toll-like receptor signaling pathway, which could lead to inflammatory effects²⁸. Mice lacking TNFAIP3 develop severe multiple organ inflamma-

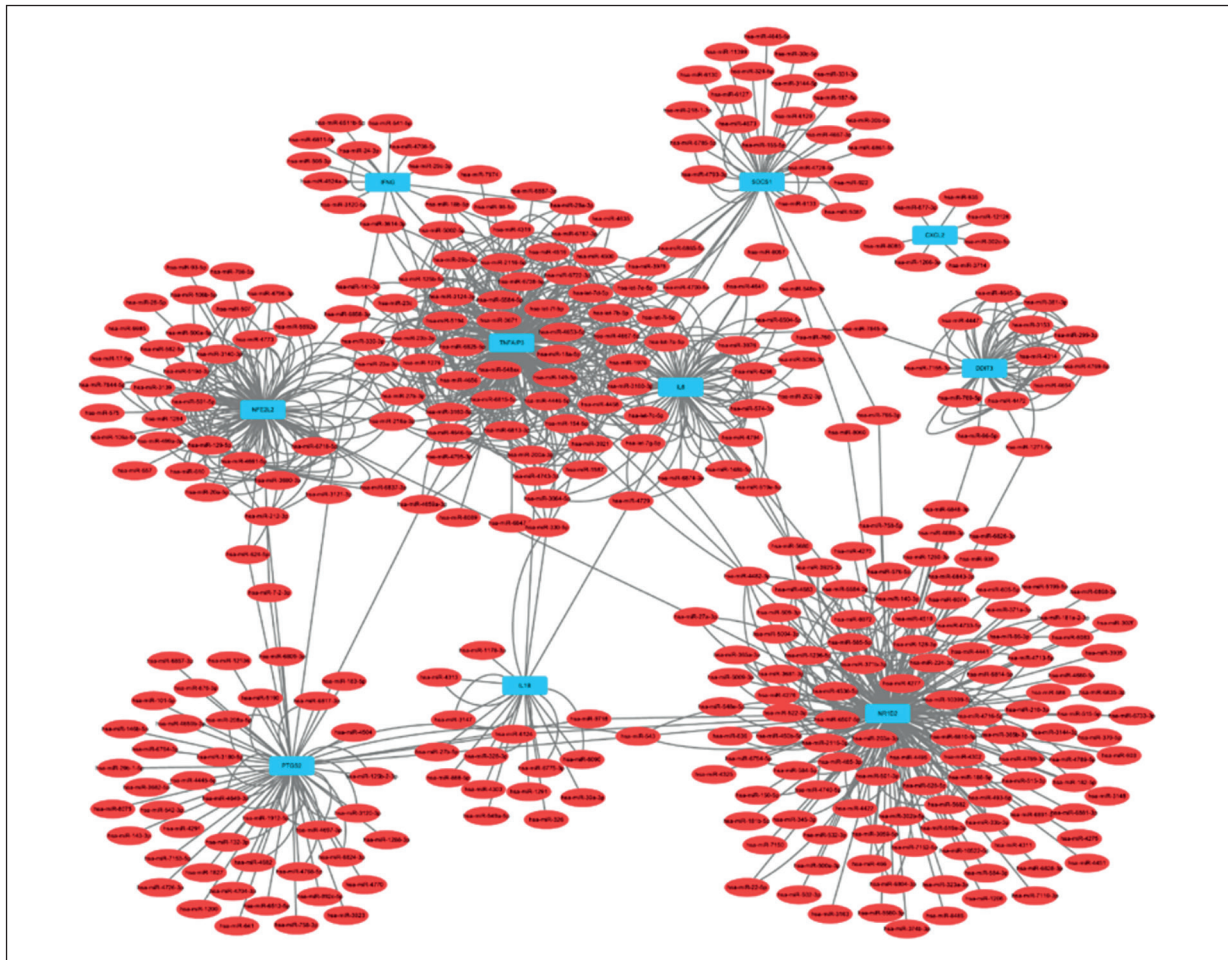


Figure 7. Predicted interactions among 10 ferroptosis-related hub genes and their target miRNAs. Blue represents 10 ferroptosis-related hub genes, and red represents the target miRNAs of 10 ferroptosis-related hub genes.

tion, leading to premature death²⁹. Likewise, in this study, TNFAIP3 was found to be involved in ferroptosis and IS.

NFE2L2, also known as nuclear factor erythroid 2-related factor 2 (Nrf2), is a transcription

factor-regulated antioxidant enzyme³⁰. It plays an important physiological role in regulating oxidative stress and inflammation. In contrast, NRF2 could regulate ferroptosis-related genes (including glutathione regulation genes) nicotin-

Table IV. Suggested top drug compounds for the hub genes of IS.

Name of drug	p-value	Adjusted p-value	Genes
Estradiol CTD 00005920	2.28E-07	2.81E-06	IL6, SOCS1, IFNG, IL1B, DDIT3, TNFAIP3, PTGS2, CXCL2, ATF3, NFE2L2
Methanol CTD 00005338	3.15E-11	1.66E-09	IFNG, IL1B, PTGS2, NFE2L2
Nsc267099 ctd 00001568	3.15E-11	1.66E-09	IL6, IFNG, IL1B, NFE2L2
Trifluoperazine PC3 UP	5.46E-15	5.88E-12	IL6, DDIT3, TNFAIP3, PTGS2, CXCL2, ATF3
Prochlorperazine PC3 UP	1.12E-12	1.72E-10	DDIT3, TNFAIP3, PTGS2, CXCL2, ATF3
Bepidil PC3 UP	1.34E-12	1.80E-10	DDIT3, TNFAIP3, PTGS2, CXCL2, ATF3
Primaquine HL60 UP	1.34E-12	1.80E-10	IL1B, DDIT3, PTGS, CXCL2, ATF3
Suloctidil PC3 UP	4.77E-14	2.05E-11	IL6, DDIT3, TNFAIP3, PTGS2, CXCL2, ATF3
Cortisol succinate CTD 00000336	1.48E-08	2.85E-07	IL6, IL1B, NFE2L2
2'-Hydroxychalcone TTD 00000428	1.48E-08	2.85E-07	IL1B, PTGS2, NFE2L2

amide adenine dinucleotide phosphate regeneration, which is critical for glutathione peroxidase 4 (GPX4) activity, and iron homeostasis³¹. Thus, Nrf2 is an important regulatory factor for ferroptosis³¹. Furthermore, one study³² revealed that Nrf2 has a neuroprotective effect through complex signal crosstalk and is located at the center of the entire pathway. The results of the present study also showed that Nrf2 is closely related to ferroptosis in elderly women with IS.

DDIT3, also called C/EBP homologous protein (CHOP), plays key roles in endoplasmic reticulum stress-induced apoptosis and autophagy³³. The expression of p53-independent p53 upregulated modulator of apoptosis, mediated by the CHOP (DDIT3) signaling pathway, is involved in the synergistic interaction between apoptosis and ferroptosis³⁴. Furthermore, CHOP (DDIT3) expression is significantly increased after 3, 6, and 12 h of reperfusion following global ischemia³⁵. These are consistent with results of our study showing that DDIT3 is closely related to ferroptosis and IS.

The main function of the *SOCS1* gene is the recruitment of E3 ubiquitin ligases to inhibit cell signaling and promote ubiquitination³⁶. However, SOCS1 is necessary for the activation of p53 and the regulation of cellular senescence, and it induces ferroptosis through p53-target genes and SLC7A11 downregulation³⁷. Exogenous SOCS1 is sufficient to adjust p53-target gene expression and make cells sensitive to ferroptosis³⁷. Another study³⁸ demonstrated that SOCS1 expression is lower in rats with IS. In summary, SOCS1 is related to ferroptosis and IS, which corresponds with our results.

IFNG, also called IFN- γ , is a dimerized soluble cytokine³⁹. Our study found that IFNG was one of the hub genes of ferroptosis in elderly women with IS. Iron and the erythropoiesis-inducing hormones (erythropoietin) affect innate immune responses by influencing IFNG-mediated iron or NF- κ B-inducible immune effector pathways in macrophages. One study⁴⁰ demonstrated that IFN- γ induces the death of human retinal pigment epithelial cells, accompanied by the main characteristics of ferroptosis. Simultaneously, treatment with IFN- γ decreases the level of GPX4, rendering cells more sensitive to ferroptosis. However, IFN- γ increases the SOD2 level in neural stem cells cultures. High-dose IFN- γ injection also aggravates the level of inflammation in a cerebral ischemic model⁴¹. In summary, IFNG (IFN- γ) is closely related to cell ferroptosis and IS, but we did not verify that IFN- γ is directly related to the ferroptosis mechanism in IS.

Another important finding is the identification of 10 potential therapeutic compounds corresponding to the 10 key genes in elderly women with IS, especially estradiol CTD 00005920. However, the influence of estrogen on stroke remains unclear. Previous scholars⁴¹ have shown that high-dose estrogen is correlated with an elevated IS risk⁴². In contrast, another study⁴² suggested that a higher dose of estrogen is not correlated with a high IS risk. Compared to estrogen, conjugated equine estrogen, comprising equine estrogens, estrone, equilin, and equilenin, is related to a high risk of stroke⁴³. Therefore, the association between estrogen and stroke risk in relation to the estrogen dose and types should thus be further investigated.

Conclusions

Based on GEO, FerrDb, and other multi-database biological big data mining, we found that *IL-6*, *IL1B*, *PTGS2*, *ATF3*, *CXCL2*, *TNFAIP3*, *NFE2L2*, *DDIT3*, *SOCS1*, and *IFNG* are ferroptosis-related DEGs that might be promising in the development of diagnostics and therapeutics for elderly women with IS. This study provides a new potential target for the clinical diagnosis of elderly women with IS. Meanwhile, the relationship between the expression of 10 key genes and therapeutic compounds suggests that estradiol could be used for the treatment of elderly women with IS. The deficiency of this study is that the key genes were not verified in our experiments. We plan to verify them in further studies.

Conflict of Interest

The Authors declare that they have no conflict of interests.

Funding

This study was supported by the National Natural Science Foundation of China (No. 81904180), Hunan Natural Science Foundation Project (No. 2018JJ3390), Changsha Science and Technology Department (No. kq1801045), and Hunan Provincial Department of education project (No. 20B429). This article has not received sponsorship for publication.

Ethics Statement

FerrDb and GEO belong to public datasets. The contributors to the database have obtained ethical approval. Thus, our research has no ethical issues or other conflicts of interest.

Availability of Data and Material

The datasets presented in this study can be found from GEO (<https://www.ncbi.nlm.nih.gov/geo/>) and FerrDb databases (<http://www.zhounan.org/ferrdb>). All data analyzed during this study are contained in this article.

Authors' Contribution

LHQ contributed to the study design and performed data analysis for the manuscript. ZY L and SL drafted the manuscript. SL contributed to data collection. All authors contributed to the article and approved the manuscript.

ORCID ID

Lihua Qin (ORCID ID: 0000-0003-3458-1520), Sheng Li (ORCID ID: 0000-0003-4827-8856), Ziyang Li (ORCID ID: 0000-0001-6674-4801).

Conflict of Interest

The Authors declare that they have no conflict of interests.

References

- 1) Akinyemi RO, Ovbiagele B, Adeniji OA, Sarfo FS, Abd-Allah F, Adoukonou T, Ogah OS, Naidoo P, Damasceno A, Walker RW, Ogunniyi A, Kalaria RN, Owolabi MO. Stroke in Africa: profile, progress, prospects and priorities. *Nat Rev Neurol* 2021; 17: 634-656.
- 2) Benjamin EJ, Blaha MJ, Chiuve SE, Cushman M, Das SR, Deo R, de Ferranti SD, Floyd J, Fornage M, Gillespie C, Isasi CR, Jiménez MC, Jordan LC, Judd SE, Lackland D, Lichtman JH, Lisabeth L, Liu S, Longenecker CT, Mackey RH, Matsushita K, Mozaffarian D, Mussolino ME, Nasir K, Neumar RW, Palaniappan L, Pandey DK, Thiagarajan RR, Reeves MJ, Ritchey M, Rodriguez CJ, Roth GA, Rosamond WD, Sasson C, Towfighi A, Tsao CW, Turner MB, Virani SS, Voeks JH, Willey JZ, Wilkins JT, Wu JH, Alger HM, Wong SS, Muntner P; American Heart Association Statistics Committee and Stroke Statistics Subcommittee. Heart Disease and Stroke Statistics-2017 Update: A Report From the American Heart Association. *Circulation* 2017; 135: e146-e603.
- 3) Samuthpongton C, Jereerat T, Suwanwela NC. Stroke risk factors, subtypes and outcome in elderly Thai patients. *BMC Neurol* 2021; 21: 322.
- 4) Seshadri S, Wolf PA. Lifetime risk of stroke and dementia: current concepts, and estimates from the Framingham Study. *Lancet Neurol* 2007; 6: 1106-1114.
- 5) Gargano JW, Reeves MJ; Paul Coverdell National Acute Stroke Registry Michigan Prototype Investigators. Sex differences in stroke recovery and stroke-specific quality of life: results from a state-wide stroke registry. *Stroke* 2007; 38: 2541-2548.
- 6) Berglund A, Schenck-Gustafsson K, von Euler M. Sex differences in the presentation of stroke. *Ma-turitas* 2017; 99: 47-50.
- 7) Qi Z, Zhao Y, Su Y, Cao B, Yang JJ, Xing Q. Serum Extracellular Vesicle-Derived miR-124-3p as a Diagnostic and Predictive Marker for Early-Stage Acute Ischemic Stroke. *Front Mol Biosci* 2021; 8: 685088.
- 8) Dixon SJ, Lemberg KM, Lamprecht MR, Skouta R, Zaitsev EM, Gleason CE, Patel DN, Bauer AJ, Cantley AM, Yang WS, Morrison B 3rd, Stockwell BR. Ferroptosis: an iron-dependent form of nonapoptotic cell death. *Cell* 2012; 149: 1060-1072.
- 9) Sampilvanjil A, Karasawa T, Yamada N, Komada T, Higashi T, Baatarjav C, Watanabe S, Kamata R, Ohno N, Takahashi M. Cigarette smoke extract induces ferroptosis in vascular smooth muscle cells. *Am J Physiol Heart Circ Physiol* 2020; 318: H508-H518.
- 10) Yu Y, Yan Y, Niu F, Wang Y, Chen X, Su G, Liu Y, Zhao X, Qian L, Liu P, Xiong Y. Ferroptosis: a cell death connecting oxidative stress, inflammation and cardiovascular diseases. *Cell Death Discov* 202; 7: 193.
- 11) Yu Y, Yan Y, Niu F, Wang Y, Chen X, Su G, Liu Y, Zhao X, Qian L, Liu P, Xiong Y. Ferroptosis: a cell death connecting oxidative stress, inflammation and cardiovascular diseases. *Cell Death Discov* 2021; 7: 193.
- 12) Gu Z, Eils R, Schlesner M. Complex heatmaps reveal patterns and correlations in multidimensional genomic data. *Bioinformatics* 2016; 32: 2847-2849.
- 13) Doms A, Schroeder M. GoPubMed: exploring PubMed with the Gene Ontology. *Nucleic Acids Res* 2005; 33(Web Server issue): W783-W786.
- 14) Walter W, Sánchez-Cabo F, Ricote M. GPlot: an R package for visually combining expression data with functional analysis. *Bioinformatics* 2015; 31: 2912-2914.
- 15) Szklarczyk D, Gable AL, Lyon D, Junge A, Wyder S, Huerta-Cepas J, Simonovic M, Doncheva NT, Morris JH, Bork P, Jensen LJ, Mering CV. STRING v11: protein-protein association networks with increased coverage, supporting functional discovery in genome-wide experimental datasets. *Nucleic Acids Res* 2019; 47: D607-D613.
- 16) Fu D, Liu H, Zhu J, Xu H, Yao J. [D-Ala2, D-Leu5] Enkephalin Inhibits TLR4/NF-κB Signaling Pathway and Protects Rat Brains against Focal Ischemia-Reperfusion Injury. *Mediators Inflamm* 2021; 2021: 6661620.
- 17) Wolinski P, Glabinski A. Chemokines and neurodegeneration in the early stage of experimental ischemic stroke. *Mediators Inflamm* 2013; 2013: 727189.
- 18) Bin S, Xin L, Lin Z, Jinhua Z, Rui G, Xiang Z. Targeting miR-10a-5p/IL-6R axis for reducing IL-6-induced cartilage cell ferroptosis. *Exp Mol Pathol* 2021; 118: 104570.

- 19) Cao Y, Li Y, He C, Yan F, Li JR, Xu HZ, Zhuang JF, Zhou H, Peng YC, Fu XJ, Lu XY, Yao Y, Wei YY, Tong Y, Zhou YF, Wang L. Selective Ferroptosis Inhibitor Liproxstatin-1 Attenuates Neurological Deficits and Neuroinflammation After Subarachnoid Hemorrhage. *Neurosci Bull* 2021; 37: 535-549.
- 20) Nadjar A, Tridon V, May MJ, Ghosh S, Dantzer R, Amédée T, Parnet P. NFκB activates in vivo the synthesis of inducible Cox-2 in the brain. *J Cereb Blood Flow Metab* 2005; 25: 1047-1059.
- 21) Chen G, Li L, Tao H. Bioinformatics Identification of Ferroptosis-Related Biomarkers and Therapeutic Compounds in Ischemic Stroke. *Front Neurol* 2021; 12: 745240.
- 22) Yang WS, SriRamaratnam R, Welsch ME, Shimada K, Skouta R, Viswanathan VS, Cheah JH, Clemons PA, Shamji AF, Clish CB, Brown LM, Girotti AW, Cornish VW, Schreiber SL, Stockwell BR. Regulation of ferroptotic cancer cell death by GPX4. *Cell* 2014; 156: 317-331.
- 23) Wang Y, Zhao Y, Ye T, Yang L, Shen Y, Li H. Ferroptosis Signaling and Regulators in Atherosclerosis. *Front Cell Dev Biol* 2021; 9: 809457.
- 24) Lu S, Wang XZ, He C, Wang L, Liang SP, Wang CC, Li C, Luo TF, Feng CS, Wang ZC, Chi GF, Ge PF. ATF3 contributes to brucine-triggered glioma cell ferroptosis via promotion of hydrogen peroxide and iron. *Acta Pharmacol Sin* 2021; 42: 1690-1702.
- 25) Wang L, Liu Y, Du T, Yang H, Lei L, Guo M, Ding HF, Zhang J, Wang H, Chen X, Yan C. ATF3 promotes erastin-induced ferroptosis by suppressing system Xc. *Cell Death Differ* 2020; 27: 662-675.
- 26) Yang R, Yao L, Du C, Wu Y. Identification of key pathways and core genes involved in atherosclerotic plaque progression. *Ann Transl Med* 2021; 9: 267.
- 27) Lodolce JP, Kolodziej LE, Rhee L, Kariuki SN, Franek BS, McGreal NM, Logsdon MF, Bartulis SJ, Perera MA, Ellis NA, Adams EJ, Hanauer SB, Jolly M, Niewold TB, Boone DL. African-derived genetic polymorphisms in TNFAIP3 mediate risk for autoimmunity. *J Immunol* 2010; 184: 7001-7009.
- 28) Hung YY, Lin CC, Kang HY, Huang TL. TNFAIP3, a negative regulator of the TLR signaling pathway, is a potential predictive biomarker of response to antidepressant treatment in major depressive disorder. *Brain Behav Immun* 2017; 59: 265-272.
- 29) Lee EG, Boone DL, Chai S, Libby SL, Chien M, Lodolce JP, Ma A. Failure to regulate TNF-induced NF-κB and cell death responses in A20-deficient mice. *Science* 2000; 289: 2350-2354.
- 30) Kensler TW, Wakabayashi N, Biswal S. Cell survival responses to environmental stresses via the Keap1-Nrf2-ARE pathway. *Annu Rev Pharmacol Toxicol* 2007; 47: 89-116.
- 31) Abdalkader M, Lampinen R, Kanninen KM, Malm TM, Liddell JR. Targeting Nrf2 to Suppress Ferroptosis and Mitochondrial Dysfunction in Neurodegeneration. *Front Neurosci* 2018; 12: 466.
- 32) Jiang S, Deng C, Lv J, Fan C, Hu W, Di S, Yan X, Ma Z, Liang Z, Yang Y. Nrf2 Weaves an Elaborate Network of Neuroprotection Against Stroke. *Mol Neurobiol* 2017; 54: 1440-1455.
- 33) Wang S, Hou P, Pan W, He W, He DC, Wang H, He H. DDIT3 Targets Innate Immunity via the DDIT3-OTUD1-MAVS Pathway To Promote Bovine Viral Diarrhea Virus Replication. *J Virol* 2021; 95: e02351-20.
- 34) Lee YS, Lee DH, Choudry HA, Bartlett DL, Lee YJ. Ferroptosis-Induced Endoplasmic Reticulum Stress: Cross-talk between Ferroptosis and Apoptosis. *Mol Cancer Res* 2018; 16: 1073-1076.
- 35) Poone GK, Hasseldam H, Munkholm N, Rasmussen RS, Grønberg NV, Johansen FF. The Hypothermic Influence on CHOP and Ero1-α in an Endoplasmic Reticulum Stress Model of Cerebral Ischemia. *Brain Sci* 2015; 5: 178-187.
- 36) Ying J, Qiu X, Lu Y, Zhang M. SOCS1 and its Potential Clinical Role in Tumor. *Pathol Oncol Res* 2019; 25: 1295-1301.
- 37) Saint-Germain E, Mignacca L, Vernier M, Bobbala D, Ilangumaran S, Ferbeyre G. SOCS1 regulates senescence and ferroptosis by modulating the expression of p53 target genes. *Aging (Albany NY)* 2017; 9: 2137-2162.
- 38) Wang XL, Qiao CM, Liu JO, Li CY. Inhibition of the SOCS1-JAK2-STAT3 Signaling Pathway Confers Neuroprotection in Rats with Ischemic Stroke. *Cell Physiol Biochem* 2017; 44: 85-98.
- 39) Gray PW, Goeddel DV. Structure of the human immune interferon gene. *Nature* 1982; 298: 859-863.
- 40) Wei TT, Zhang MY, Zheng XH, Xie TH, Wang W, Zou J, Li Y, Li HY, Cai J, Wang X, Tan J, Yang X, Yao Y, Zhu L. Interferon-γ induces retinal pigment epithelial cell Ferroptosis by a JAK1-2/STAT1/SLC7A11 signaling pathway in Age-related Macular Degeneration. *FEBS J* 2022; 289: 1968-1983.
- 41) Zhang G, Chen L, Chen W, Li B, Yu Y, Lin F, Guo X, Wang H, Wu G, Gu B, Miao W, Kong J, Jin X, Yi G, You Y, Su X, Gu N. Neural Stem Cells Alleviate Inflammation via Neutralization of IFN-γ Negative Effect in Ischemic Stroke Model. *J Biomed Nanotechnol* 2018; 14: 1178-1188.
- 42) Løkkegaard E, Nielsen LH, Keiding N. Risk of Stroke with Various Types of Menopausal Hormone Therapies: A National Cohort Study. *Stroke* 2017; 48: 2266-2269.
- 43) Chang WC, Wang JH, Ding DC. Conjugated equine estrogen used in postmenopausal women associated with a higher risk of stroke than estradiol. *Sci Rep* 2021; 11: 10801.